Earth Planets Space, **65**, 645–655, 2013

Transition in eruption style during the 2011 eruption of Shinmoe-dake, in the Kirishima volcanic group: Implications from a steady conduit flow model

Ryo Tanaka and Takeshi Hashimoto

Institute of Seismology and Volcanology, Faculty of Science, Hokkaido University, N10W8, Kita-ku, Sapporo, Hokkaido 060-0810, Japan

(Received October 30, 2012; Revised April 10, 2013; Accepted May 4, 2013; Online published July 8, 2013)

Mount Shinmoe-dake, in the Kirishima volcanic group (in southern Kyushu, Japan), erupted in January 2011. The eruption style was initially phreatomagmatic, and then underwent a series of transitions from sub-plinian explosions to an extrusion of lava from the summit crater. The purpose of the present study is to investigate the cause of such changes in eruption styles, focusing on the conditions for the eruption to be non-explosive and for the lava effusion to cease. To examine the conditions in the conduit and magma chamber, a numerical code is devised, based on the one-dimensional steady flow model of Kozono and Koyaguchi (2010), who modeled a dome-forming eruption. We systematically search for a condition in which the magma would not be fragmented, but the initial volatile content in the magma chamber would remain constant and unchanged. We find that the high magma permeability and/or the high degree of lateral gas escape was needed for the eruption to be effusive, and we estimate the pressure decrement at the cessation of lava extrusion.

Key words: Conduit-flow model, Shinmoe-dake, eruption, volcano, eruption style, permeability, degassing, magma chamber.

1. Introduction

The Kirishima volcanoes, located on the border between Kagoshima and Miyazaki prefectures, southern Kyushu, Japan, consist of approximately 20 Quaternary volcanic edifices that trend in a roughly NW-SE direction. Shinmoe-dake, one of the youngest volcanoes, is located in the middle of this chain (Fig. 1 shows the location of the volcano). Shinmoe-dake has been volcanically active since ca. 10 ka. Historically it has erupted repeatedly and violently, and has now reached its present height of 1,421 m above sea level (Imura and Kobayashi, 2001).

Recent eruptions took place in 1716–1717 (the Kyoho eruption), 1822, 1959, 1991, 2008, and 2011. Among these events, the Kyoho eruption was the largest, with an eruption style that changed from phreatic to phreatomagmatic, with a final magmatic explosion. All the other eruptions before 2011 were phreatic (Imura and Kobayashi, 2001; Tsutsui *et al*., 2005).

On January 19, 2011, Shinmoe-dake resumed activity, beginning with a small phreatomagmatic explosion and evolving into three successive sub-plinian eruptions on January 26 and 27, which were accompanied by pumice falls (Nakada *et al*., 2013). The sub-plinian stage lasted no longer than two days, and the three explosive events produced ejected material of 1.2–1.6 $\times$ 10^7 m^3 DRE (Dense Rock Equivalent) (Kozono *et al*., 2013). A lava dome with a diameter of some tens of meters was identified from helicopter observations on January 28 (Nakada *et al*., 2013). By January 31, the dome had filled the summit crater (Nakada *et al*., 2013), but no further growth was observed on February 1. The extruded volume of the lava dome over the four days (Jan. 28–31) amounted to 1.2–1.5 $\times$ 10^7 m^3 DRE (Kozono *et al*., 2013). The eruption style then became vulcanian and subsequent vigorous explosions took place until February 2011. Thereafter the surface activity of Shinmoe-dake gradually abated (Fig. 2 summarizes the eruptions of Shinmoe-dake in historic times and the sequence of the major eruptions in 2011).

Several key parameters have been measured or estimated from visual and geophysical observations, such as observations of the timing, duration and volumetric discharge rate of the eruption, as well as the location of the magma chamber; hence, the eruption of 2011 is a suitable example for a quantitative examination using physical models of magma flow in a conduit. Other important parameters related to the property of the magma have also been estimated for this event from mineralogical and petrological studies.

A quantitative discussion regarding the state within the conduit and the magma chamber is important in considering subsequent eruption scenarios, since it is known that the mechanism and efficiency of the escape of gas from the conduit control the eruption style. Previous studies on steady-state conduit flow models suggest the use of two degassing mechanisms to describe non-explosive dome-forming eruptions. One mechanism is a volatile loss through the conduit walls (e.g., Eichelberger *et al*., 1986; Jaupart and Allegre, 1991; Woods and Koyaguchi, 1994), while the other is vertical gas escape, wherein the melt and gas ascend at different velocities (e.g., Melnik and Sparks, 1999; Yoshida and Koyaguchi, 1999; Kozono and Koyaguchi, 2010). In both of these mechanisms, the efficiency of outgassing is subject

doi:10.5047/eps.2013.05.002

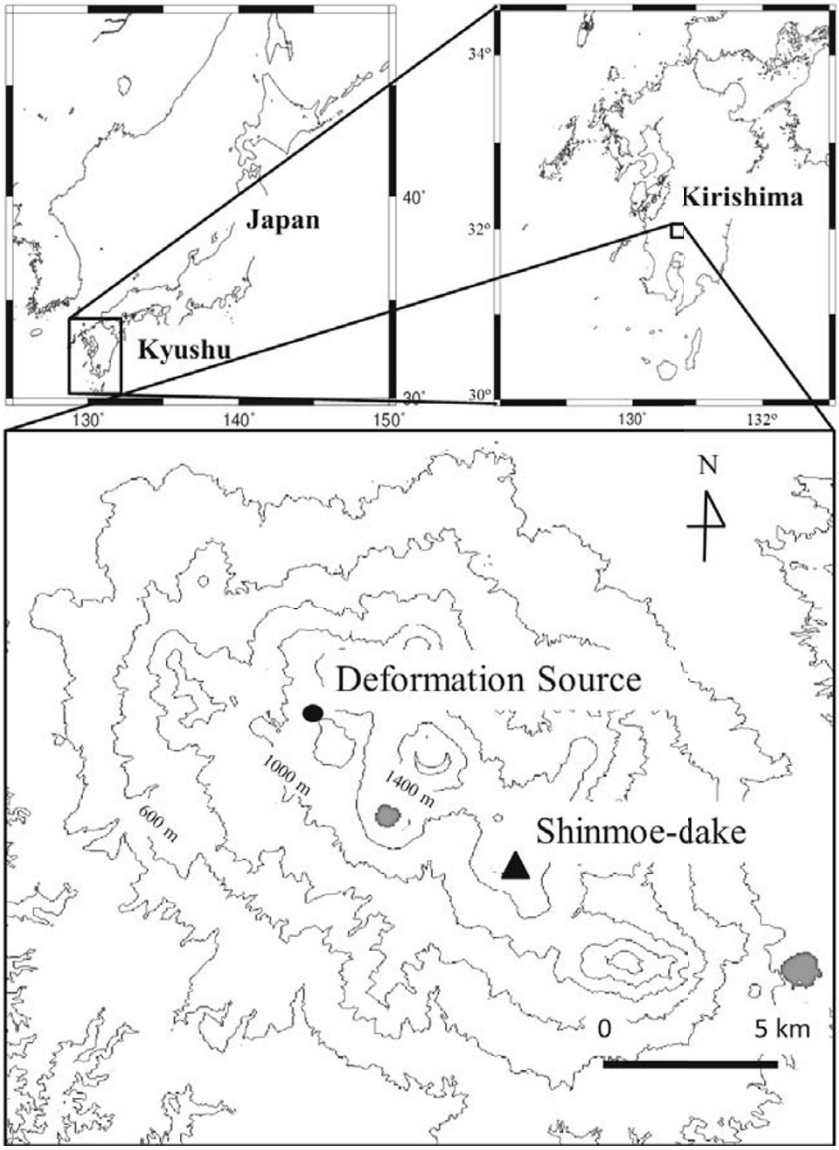

Fig. 1. Location of Shinmoe-dake, Kirishima volcanic group.

to common parameters such as the radius of the conduit, magma viscosity, bubble size, and the permeability of the wall rock and magma itself. In this study, we take particular note of the permeability of magma, which we believe has a significant effect on the result. An empirical relationship between permeability and the porosity of magma has been systematically investigated by Mueller *et al*. (2005) in relation to various volcanic rocks. We apply this empirical relationship to the one-dimensional (1D) conduit flow, in order to evaluate a possible condition that caused the eruption of Shinmoe-dake 2011 to experience a non-explosive stage. We also consider the results of certain preceding studies on steady-state conduit flow models that have suggested that the pressure change in the magma chamber largely contributes to the initiation and termination of an eruption (e.g., Melnik and Sparks, 1999; Barmin *et al*., 2002). Using the 2011 eruption of Shinmoe-dake as an example, and by examining the dependency of the magma discharge rate on the chamber pressure, we consider how a change in the chamber pressure contributes to the termination of the effusive eruption. In addition, we also discuss the cause of the transition from sub-plinian to effusive eruptions.

2. Governing Equations and Numerical Calculations

In this study, we investigate the effusive stage of the 2011 Shinmoe-dake eruption by means of numerical calculations based on the 1D steady conduit flow model. We calculate porosity profiles of upwelling magma along the conduit under various conditions, in order to search the ranges of parameters that make the porosity smaller than the fragmentation criterion at any depth. We then demonstrate the basic ideas of the model, including details of the governing equations, before presenting the results of calculations.

We assume that magma fragmentation in the conduit arises only when porosity exceeds a threshold level of 0.75 (Proussevitch *et al*., 1993), above which bubble suspensions of a uniform size in the melt cannot maintain a spherical shape. The adequacy of the criterion is discussed in Section 4. We used the 1D steady-state model, based on Ko-

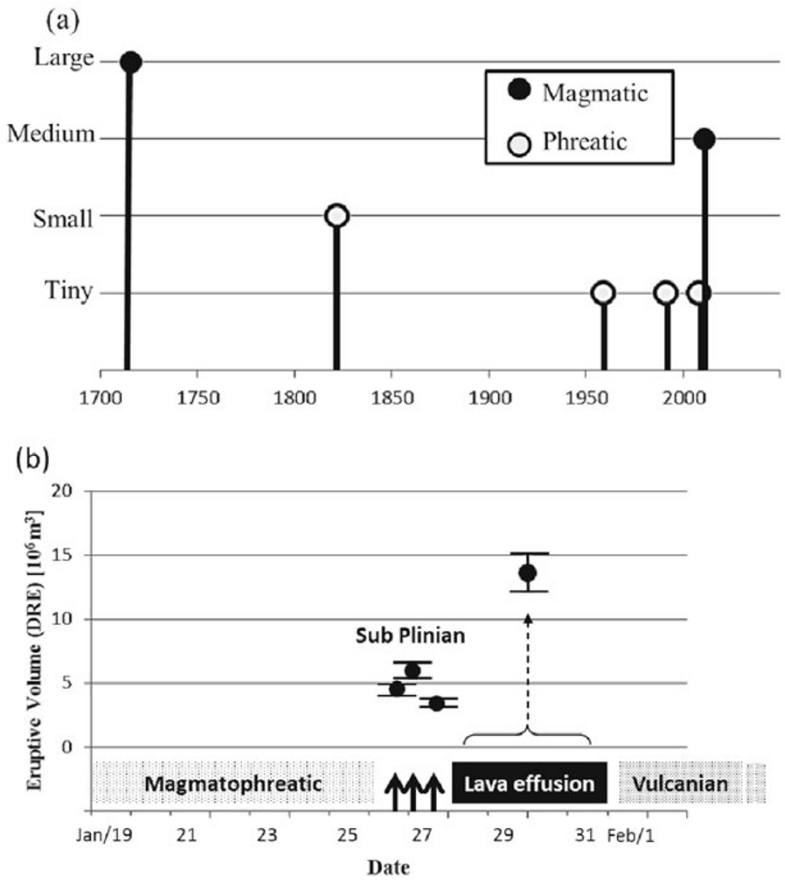

Fig. 2. (a) Major eruptions of Shinmoe-dake in historic times. (b) Time sequence and eruptive volume in the early stage of the 2011 eruption. Short solid arrows represent the timing of three sub-plinian eruptions. Dashed line indicates the period of lava extrusion. Circles with error bars represent the eruptive volume in DRE for each event (Kozono *et al*., 2013). For the lava effusion stage, the total volume is shown.

zono and Koyaguchi (2010), to calculate the porosity profile along the conduit. The model of Kozono and Koyaguchi (2010) is designed for a dome-forming eruption, unlike the model of Wilson *et al*. (1980) in which an explosive eruption is supposed. We need to use a non-explosive model to deal with an effusive stage of the eruption of Shinmoe-dake. In addition, the model of Kozono and Koyaguchi (2010) is more straightforward and simpler in calculating the magma viscosity than another representative effusive model by Melnik and Sparks (1999), in which a more complex process related to crystal growth kinetics is taken into account.

In the model of Kozono and Koyaguchi (2010), isothermal magma ascends through a cylindrical conduit with a constant radius. The vertical relative motion between the gas and liquid phases (i.e., vertical gas escape) is taken into account. As the magma ascends from a depth, the flow regime shifts from bubbly to permeable. Such a transition in the flow regime influences the interaction forces between gas and liquid. In order to describe this effect exactly, it is necessary to consider two separate constitutive laws for the interaction force. Instead, we treat the flow regime as permeable throughout the conduit's entirety. Regardless of this simplification, no discernible deviation from the example shown in Kozono and Koyaguchi (2010) is found in the calculated porosity profile. This is probably because the relative velocity between gas and liquid is extremely low in a low-porosity-region for either of the flow regimes, so that the difference is negligible. The basic equations from the above model are expressed as follows:

$$\rho_l u_l (1-\phi) = (1-n)q, \tag{1}$$

$$\rho_g u_g \phi = nq(1-E_w), \tag{2}$$

$$\rho_l u_l (1-\phi)\frac{du_l}{dz} = -(1-\phi)\frac{dP}{dz} - \rho_l(1-\phi)g - F_{lw} + F_{lg}, \tag{3}$$

$$\rho_g u_g \phi \frac{du_g}{dz} = -\phi\frac{dP}{dz} - \rho_g \phi g - F_{lg}, \tag{4}$$

$$P = \rho_g RT, \tag{5}$$

$$n = \frac{n_0 - s\sqrt{P}}{1 - s\sqrt{P}}, \tag{6}$$

$$q = \frac{\Delta \dot{V}_{ex}\rho_l}{R_c^2 \pi}. \tag{7}$$

Equations (1) and (2) represent mass conservation for the liquid and the gas phases, respectively. Here, ρ_l and ρ_g represent the density of the liquid and the gas, respectively; u_l and u_g are the vertical velocities of the liquid and the gas, respectively; q is the mass that crosses the unit cross-sectional area in unit time (mass flow rate); ϕ is the volume fraction of the gas phase; n, defined in Eq. (6), is the gas

Table 1. Parameters for Shinmoe-dake 2011 eruption.

Parameters	Value range	References
Lava discharge rate	70–87 m^3/s	Kozono *et al*. (2013)
Magma Temperature	960–980°C	Suzuki *et al*. (2013)
Initial H_2O content	4 wt%	Suzuki *et al*. (2013)
Volume fraction of phenocrysts	30%	Suzuki *et al*. (2013)
Magma chamber depth	6.2 km	GSI (2012)

Table 2. Constants used in this study.

Constants	Symbol	Value	References
Density of liquid	ρ_l	2500 kg/m^3	—
Gravity acceleration	g	9.8 m/s^2	—
Gas constant	R	462 J kg^{-1} K^{-1}	—
Saturation constant	s	4.11×10^{-6} $Pa^{-1/2}$	—
Viscosity of gas	μ_g	10^{-5} Pa s	—
Permeability constant	k_0	1×10^{-17} m^2	Mueller *et al*. (2005)

mass-flow-rate fraction; n_0 represents the initial H_2O content. P is the pressure of the magma; and s is the saturation constant. In Eq. (2), we introduce lateral gas escape through the conduit wall, by forcing the reduction of the gas phase from each depth. During this stage, the rate of lateral gas escape at each depth is obtained by multiplying the total gas flow rate nq by E_w, the ratio of the lateral gas flow rate to the total gas flow rate. Equations (3) and (4) describe momentum conservation for the liquid and the gas, respectively. F_{lw} is the friction force between the liquid and the conduit wall, while F_{lg} is the interaction force between the liquid and the gas. Equation (5) describes the state for the gas phase, in which R and T are the gas constant for H_2O (462 J kg^{-1} K^{-1}) and the magma temperature, respectively. Since we assume the magma temperature to be constant, the energy equation is not solved. Equation (7) calculates the mass flow rate using the discharge rate $\Delta\dot{V}_{ex}$ and the conduit radius R_c.

In accordance with Wilson *et al*. (1980), we represent the effect on the liquid from the friction from the conduit wall, as shown in Eq. (8):

$$F_{lw} = \frac{8\mu}{R_c^2} u_l, \tag{8}$$

where μ is the magma viscosity. To be exact, it is more appropriate to use the viscosity for the mixture of liquid and gas for μ, since Eq. (8) is derived from the Poiseuille flow. However, we followed a similar procedure to that of Kozono and Koyaguchi (2010) in calculating μ, in which the dissolved H_2O and crystal contents are taken into account.

In a permeable flow, F_{lg} is expressed as follows:

$$F_{lg} = \frac{\mu_g}{k} \phi^2 (u_g - u_l), \tag{9}$$

where μ_g and k represent the gas viscosity and permeability of magma, respectively. According to Mueller *et al*. (2005), k is given as:

$$k = k_0 (100\phi)^{\omega}, \tag{10}$$

where k_0 is a constant ($= 1 \times 10^{-17}$ m^2) and the exponent parameter ω ranges from 3.0 to 3.8, as estimated in the experiments of Mueller *et al*. (2005). As ω increases, so does the efficiency of the vertical gas escape, and vice versa. Tables 1 and 2 list the parameters and constants used in our calculations.

In the case of the 2011 event, the injection of hot magma into a shallower chamber at a depth of 5 km (=125 MPa) with a lower temperature has been suggested from the petrological study by Suzuki *et al*. (2013). In the following calculations, we refer to Suzuki *et al*. (2013) for the parameters such as the temperature, the initial water content, and the volume fraction of phenocrysts.

Since the accurate conduit size is not known, we introduced a range of radius, from 5 m to 20 m, based on the first eyewitness' observation of the lava dome on January 28 (Nakada *et al*., 2013). With respect to the depth of the magma chamber, we refer to a joint analysis of GPS (Global Positioning System) data by the Geospatial Information Authority of Japan (GSI), the National Research Institute for Earth Science and Disaster Mitigation (NIED), and the Japan Meteorological Agency (JMA). According to the joint analysis, the depth of a co-eruptive deflation source was reported by GSI (2012) as being 6.2 km. All the estimates for the geodetic source depth (GSI, 2012; Kozono *et al*., 2013; Nakao *et al*., 2013; Ueda *et al*., 2013) are deeper than the shallower magma chamber of the hot magma. We assume the deeper magma chamber to be the lower boundary. We do not take into account the existence of the shallow magma chamber in the conduit flow calculation, but the magma flowing in the conduit is assumed to be the mixed magma generated at the shallower magma chamber (Suzuki *et al*., 2013). Because no significant change in the deformation source is reported during the eruption, we commonly use 6 km as the conduit length in the present paper. However, considering an argument by Slezin (2003) which discussed the critical conduit length in relation to an eruption style, we examined the effect of the conduit length by changing it from 5 to 7 km, before undertaking specific calculations. Such a change does not significantly affect the calculation results, because the level of the exsolution is shallow.

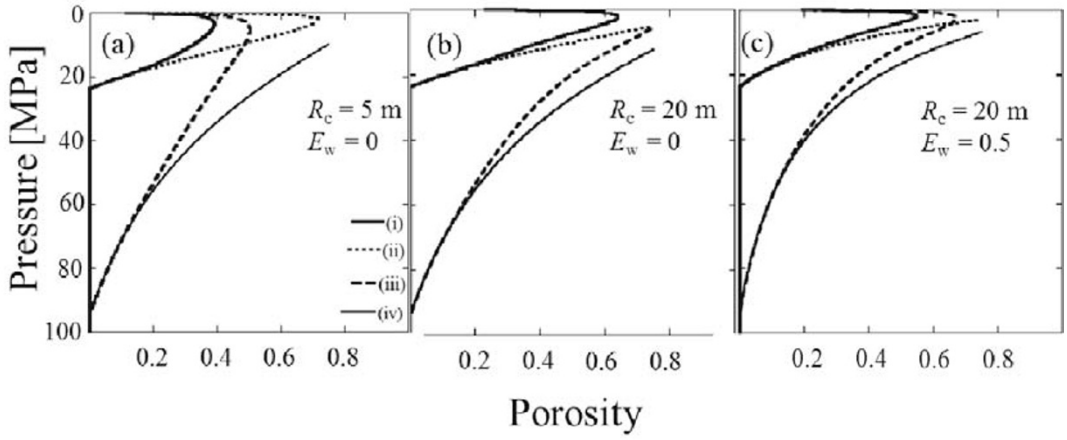

Fig. 3. Representative porosity profiles versus pressure along the conduit between the magma chamber and the vent. Panel (a): Conduit radius, $R_c = 5$ m; Fraction of lateral gas escape, $E_w = 0$. Panel (b): $R_c = 20$ m; $E_w = 0$. Panel (c): $R_c = 20$ m; $E_w = 0.5$. Parameters used in the calculations are $T = 980^{\circ}$C and discharge rate = 87 m^3/s for all lines. (i) $n_0 = 2.0$ wt%, $\omega = 3.8$, (ii) $n_0 = 2.0$ wt%, $\omega = 3.0$, (iii) $n_0 = 4.0$ wt%, $\omega = 3.8$, (iv) $n_0 = 4.0$ wt%, $\omega = 3.0$.

3. Results

3.1 Porosity profile

Figure 3 shows several examples of the porosity profile along the conduit, calculated by solving the differential equations (1)–(10) as a two-point boundary value problem. The pressure at the bottom and the top are those in the magma chamber and the atmosphere, respectively. The calculation is stopped when the porosity exceeds a critical void fraction, ϕ_c at any depth, since this indicates the occurrence of magma fragmentation and no dome-forming eruption. We show three cases: (a) narrow conduit without lateral degassing; (b) wide conduit without lateral degassing; (c) wide conduit with lateral degassing. Four lines in each panel correspond to the conditions: (i) $n_0 = 2.0$ wt%, $\omega = 3.8$; (ii) $n_0 = 2.0$ wt%, $\omega = 3.0$, (iii) $n_0 = 4.0$ wt%, $\omega = 3.8$; (iv) $n_0 = 4.0$ wt%, $\omega = 3.0$. For three of the four lines in panel (b), magma fragmentation occurs at a pressure around 10 MPa, which leads to an explosive eruption. In contrast, three of the four lines in panel (a) meet the requirement of a non-explosive eruption without fragmentation, in which a larger friction force F_{lw} from the narrower conduit wall hinders the ascent of the liquid phase. A large F_{lw} promotes the efficiency of vertical degassing as a result of an enhanced relative velocity between the gas and the liquid phases, because the velocities for each phase are controlled by Eqs. (3) and (4). Meanwhile, an explosive regime represented by line (iii) in panel (b) turns into non-explosive in panel (c) as a result of introducing lateral degassing. As inferred from these simple examples, the occurrence of magma fragmentation depends on parameters such as the conduit width, the temperature of the magma, the amount of crystals, and the initial volatile content. In our calculations, we use realistic parameters of the actual lava effusion stage in the 2011 eruption (Table 1), based on observations or material analyses. We calculate the porosity profile of the magma along the conduit and look for acceptable ranges of the conduit radius R_c, the fraction of the lateral gas flow rate E_w, and the permeability exponent ω.

3.2 Magma permeability

For the magma flowing in a conduit to reach the surface of the ground without fragmentation, ω in Eq. (10), (the exponent of the porosity-permeability relationship), should be large enough to realize an effective gas escape from the system. Figure 4 shows the lower bound of ω, mapped with respect to the conduit radius and the degree of lateral degassing, below which the magma will be fragmented at some depth. We denote here the lower bound as ω_c. In the present study, we refer to the fragmentation criterion based on the critical void fraction, ϕ_c of 75% (Fig. 4(a)). Other cases in which ϕ_c is 70% (Fig. 4(b)) or 80% (Fig. 4(c)), are also shown for reference.

With relation to the effect of a conduit width under a fixed fraction of lateral gas escape, we recognize that when the conduit is wider, the values of ω_c are larger. This is explained by the effect of wall friction, as has been discussed with Fig. 3. When the friction of the conduit wall is small, the relative velocity between the liquid and the gas is also small, and as a result, the efficiency of vertical gas escape is reduced. To suppress the magma fragmentation under such conditions, an efficient degassing through a higher permeability is required. In this respect, looking at the variation with respect to the fraction of the lateral gas escape for a given conduit radius, a smaller ω_c is found for the system with a higher contribution of lateral degassing. In other words, even if the efficiency of vertical gas escape is small, magma can ascend without fragmentation in a conduit where lateral degassing is ensured, as has already been presented in previous studies (e.g., Woods and Koyaguchi, 1994).

We do, however, note a situation in which the degree of the lateral degassing E_w is zero (i.e., the gas escapes only vertically). In the numerical calculations shown by Kozono and Koyaguchi (2010), ω is assumed as a constant value of 3.0. Applying the same assumption to the present case for the 2011 eruption inevitably results in magma fragmentation (i.e., $\omega < \omega_c$) (for a conduit radii R_c of 5 to 20 m), if no lateral gas escape is introduced (see the extreme left

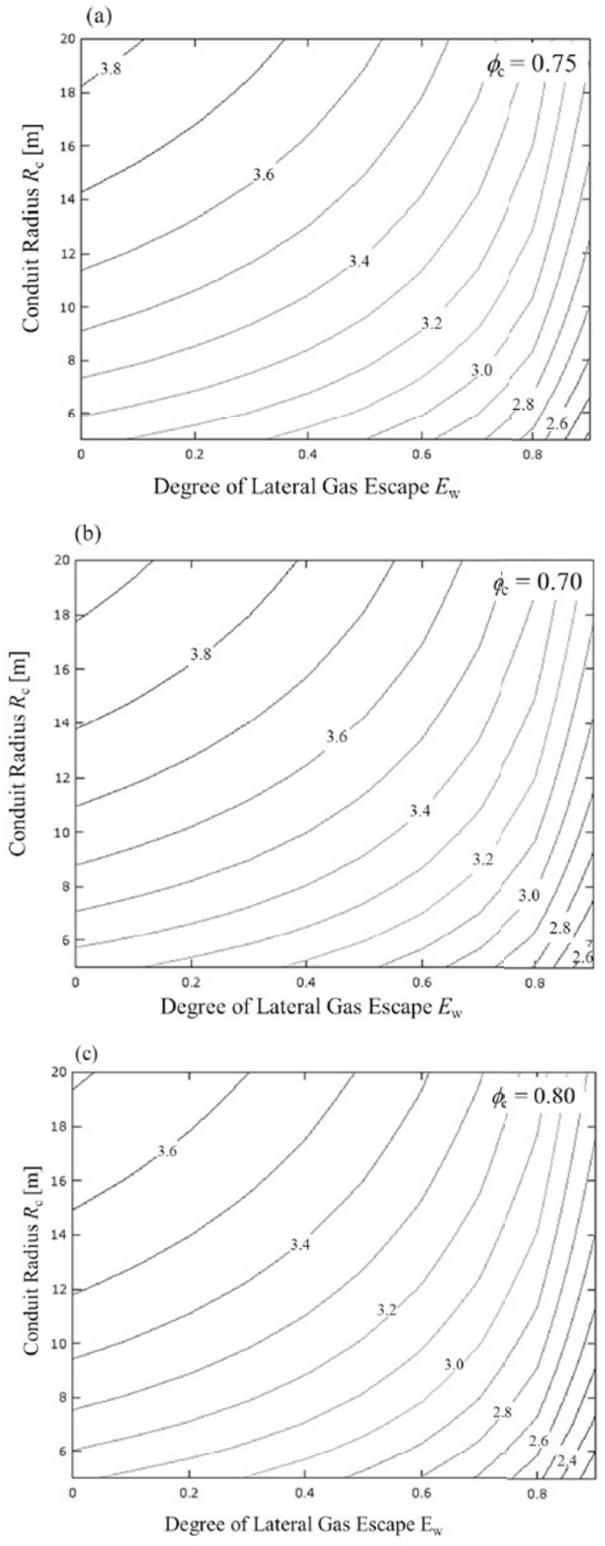

Fig. 4. Critical permeability exponent ω_c as a function of R_c and E_w, below which magma is fragmented at some depth in the conduit. Common parameters are $T = 980^{\circ}$C, $n_0 = 4.0$ wt%, $L = 6$ km, discharge rate $= 87$ m^3/s. (a) Critical gas volume fraction 75%, (b) 70% and (c) 80%.

of Fig. 4(a)). Mueller *et al*. (2005) also proposed a possible range for ω to be between 3.0 and 3.8, based on their laboratory experiments on several rock species. Figure 4(a) indicates that introducing such an allowance range for ω greatly relaxes the condition. It suggests that magma in the dome-forming stage of the 2011 eruption may have reached the surface without fragmentation; even if it was not accompanied by lateral degassing. For simplicity, in the following calculations we adopt a model without lateral gas escape. The plausibility of this assumption will be discussed later.

3.3 Magma chamber pressure during lava extrusion

The relation between the discharge rate and the magma chamber pressure P_0 is obtained from a compilation of numerical calculations, under a condition where there is no magma fragmentation in a conduit. Figures 5(a) and 5(b) show the relation between the volumetric discharge rate and the chamber pressure, with the permeability exponent ω and the conduit radius R_c as parameters, respectively. In these calculations, other parameters such as the conduit length L, magma temperature T, and initial water content n_0, are fixed values listed in Tables 1 and 2. In Fig. 5(a), an increase in ω brings about the rightward shift of the solution curves, especially around the points of minimum chamber pressure which correspond to a moderate discharge rate. Since it is difficult to further constrain the value of ω, we refer to the most relaxed condition ($\omega = 3.8$) in the following calculations. Meanwhile, dependence on the conduit radius mainly appears in the upper half of the solution curves, as shown in Fig. 5(b). For a discharge rate of higher than 10 m^3/s, a larger conduit results in a leftward shift of the solution curves. However, the lower half of the diagram is not significantly affected by R_c.

In general, there can be multiple steady solutions of the discharge rate which satisfy the given L and P_0 (Melnik and Sparks, 1999; Kozono and Koyaguchi, 2009). All the curves in Fig. 5 are multi-valued functions of P_0, suggesting that the magma-conduit system of Shinmoe-dake also has multiple steady solutions for a given chamber pressure. On the other hand, these curves are single-valued functions with respect to the discharge rate. Once a discharge rate is obtained from observation, the chamber pressure that meets the discharge rate is uniquely determined for each curve. In the case of the lava extrusion in the 2011 event, the discharge rate is 87 m^3/s (Kozono *et al*., 2013). The dashed line in Fig. 5(b) indicates this observed discharge rate, and the intersection with each curve gives the corresponding chamber pressure. We consider that the chamber pressure should not be very different from the lithostatic pressure of the host rock, because the wall of a magma chamber could collapse if the pressure gap exceeds the tensile strength of the wall rock (Wilson *et al*., 1980). Hence, we assume here that the chamber pressure was balanced to that of the lithostatic pressure at the beginning of the lava effusive stage, and is, therefore, calculated as being 1.5×10^8 Pa at a depth of 6 km, given that the density of the crust is 2,500 kg/m^3. Accordingly, we find the solution with a conduit radius of 16 m to be the most fitting of the solutions shown in Fig. 5(b).

3.4 Magma chamber pressure at the termination of lava extrusion

In general, an unsteady treatment is necessary when we consider a time-dependent phenomenon. However, if the duration of an eruption is sufficiently longer than the ascent time of the magma through a conduit, the processes may

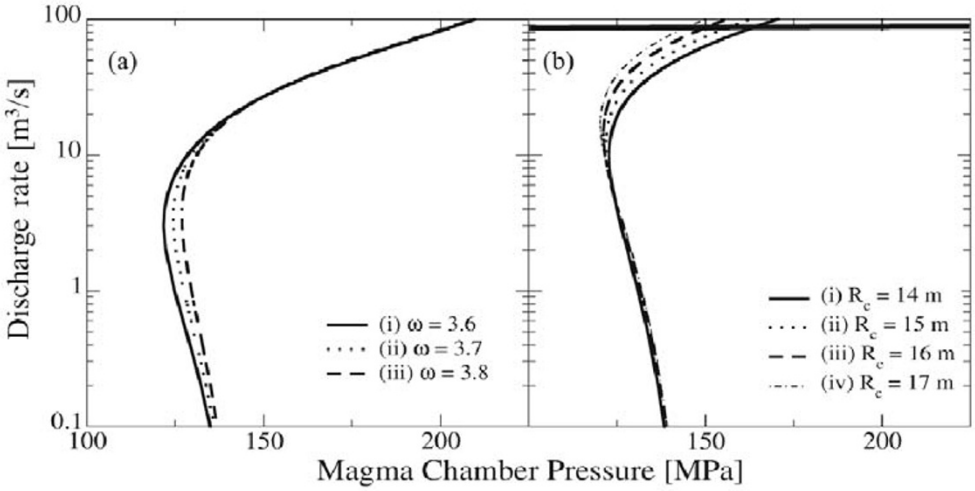

Fig. 5. Relation between the magma chamber pressure and volumetric discharge rate in the steady solutions without fragmentation. (a) Variations with the permeability exponent, ω. Other parameters are fixed as $R_c = 10$ m, $T = 980^\circ$C, $n_0 = 4.0$ wt%, $L = 6$ km, $E_w = 0$. (b) Variations with conduit radius, R_c. Other parameters are fixed as $\omega = 3.8$, $T = 980^\circ$C, $n_0 = 4.0$ wt%, $L = 6$ km, $E_w = 0$. Dashed line indicates the observed discharge rate (87 m^3/s) for the lava extrusion stage.

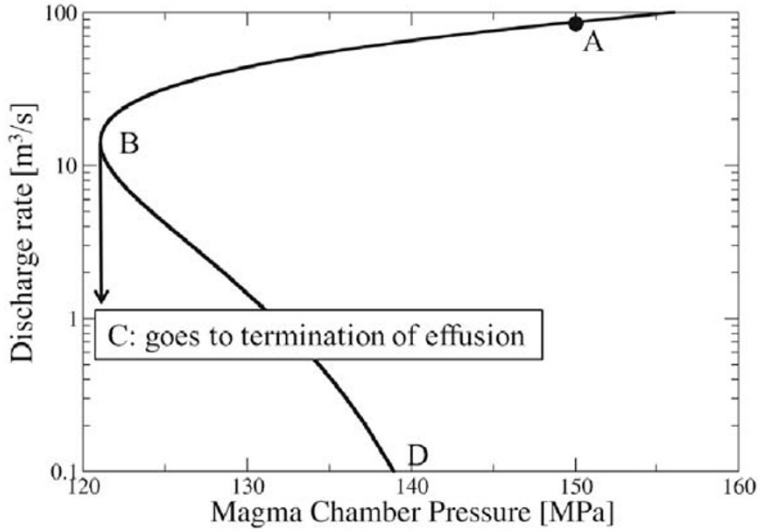

Fig. 6. Relation between the magma chamber pressure and volumetric discharge rate in the most likely steady solution for the lava extrusion stage of the 2011 event. Point A corresponds to the initiation of lava effusion at which the discharge rate is 87 m^3/s.

be approximated by a steady model. In the present case, the ascent velocity of the liquid phase is 0.1 m/s (discharge rate = 87 m^3/s, $R_c = 16$ m). The time required for the magma to travel from the chamber to the surface of the ground is therefore approximately 0.7 days, which is 5 to 6 times shorter than the duration of the lava extrusion stage (4 days). Although they do not differ by an order, we consider the processes in the conduit can be regarded as quasi-stationary.

Figure 6 shows the steady solution curve under the most likely parameters ($\omega = 3.8$, $R_c = 16$ m), based on the discussion in the previous section. The upper part of the tortuous curve demonstrates a positive dependence of the discharge rate on the chamber pressure (point A to B), and, in contrast, a negative dependence is seen along the lower part of the diagram (point B to D). This negative dependence is considered to be caused by the denser, and less porous, magma column, due to an effective gas escape in the low-discharge-rate region, in which a higher chamber pressure is required to keep such dense magma flowing upward against gravity. The cause of this negative dependence is also discussed by Melnik and Sparks (1999).

Let us now consider the time evolution of the solution in Fig. 6. Lava starts to effuse at the observed eruption rate of 87 m^3/s, and at an estimated magma chamber pressure of 1.5×10^8 Pa (point A). This is a steady solution, and, hence, no solution shift occurs as long as the boundary conditions stay unchanged. In real cases, however, the discharge rate steadily decreases toward point B, as does the chamber pressure because the chamber volume is finite. There are no steady solutions in the left-hand side of point B. After that, the processes must depart from a steady regime and further decrease in the chamber pressure due to ejection of magma inevitably results in the cessation of

the eruption (i.e., the discharge rate goes to zero). The behavior of the system in the final processes is out of the framework of the present modeling. Qualitatively, extreme slow-down of the liquid phase, complete out-gassing in the conduit, compaction of the magma column, subsequent repressurization of the chamber (e.g., due to partial drain back), and achievement of a new pressure balance between the chamber and the denser magma column (i.e., another steady state with zero-flux), is a likely scenario. Since we assume the density of the crust to be 2,500 kg/m^3, the final magma chamber pressure is also balanced to the lithostatic pressure. Accordingly, the magma chamber pressure at the termination of the lava extrusion is virtually regarded as the pressure at point B (i.e., 1.2×10^8 Pa). Therefore, the amount of pressure decreasing within the magma chamber, from the start to the end of lava effusion, is estimated to be 3×10^7 Pa.

4. Discussion

4.1 Transition from sub-plinian eruption to lava extrusion

We consider here the controlling factor for the transition from a sub-plinian eruption to lava extrusion. First, we examine whether a reduction of the H_2O content of the magma can explain the transition from explosive to effusive eruptions. This examination is based on the somewhat intuitive idea that the explosivity of the chamber magma might have become lost in the course of sub-plinian explosions, causing the eruption style to be switched to an effusive one. A series of calculations revealed that in order to suppress magma fragmentation, it was necessary for the H_2O content in the magma chamber to have decreased from 4 wt% to about 1 wt%, (in which $\omega = 3.0$ and the observed temperature and discharge rate are used). However, there is no supporting evidence from petrological studies to suggest such remarkable changes in the magmatic H_2O content with time. In addition, Suzuki *et al*. (2013) have shown that the mineral composition of the ejecta in 2011 stayed unchanged before and after the sub-plinian stage. Therefore, it is unlikely that the water content in the magma chamber experienced a significant reduction in the course of the eruption. Since the property of the magma did not significantly change with time, the transition from sub-plinian to lava extrusion phases needs another explanation. The most plausible one is the jump in the mass flow rate between multiple steady solutions within a common chamber pressure, in which one corresponds to explosive and the other to effusive. We expect that such a jump occurred. However, this cannot be confirmed by our modeling as it does not deal with an explosive regime.

4.2 Fragmentation criteria

In this study, we primarily introduced the fragmentation criterion of Proussevitch *et al*. (1993), with the critical gas fraction being 0.75. Let us discuss here how a change in this critical value affects the results. Figures 4(b) and 4(c) show the ω_c for a given conduit radius and the degree of lateral degassing, when ϕ_c is 0.7 and 0.8, respectively. In either case, the condition ($\omega_c < 3.8$) covers a fairly wide range in E_w and R_c, and suggests that the critical void fraction does not essentially affect the present discussion.

We also examine another fragmentation criterion: Papale (1999) proposed fragmentation based on the strain rate. He considered that a critical value of the strain rate for the flowing magma in the conduit is on the border of a brittle-ductile transition. Using this criterion, magma fragments when the following condition is satisfied:

$$\frac{du_l}{dz} > \kappa \frac{G_\infty}{\mu}, \tag{11}$$

where G_∞ represents the elastic modulus at infinite frequency, ranging from 2.5 to 30 GPa. κ is a coefficient which is determined experimentally as 0.01 (Dingwell and Webb, 1989; Webb and Dingwell, 1990). Figure 7 shows the profiles of the strain rate and the critical strain rate (right-hand-side of Eq. (11)) along the conduit. It is clear from the figure that the strain rate is far below the fragmentation criterion at any depth. In summary, the conditions we considered in Figs. 5 and 6 are below the fragmentation criteria of Proussevitch *et al*. (1993) and Papale (1999).

4.3 Inclined conduit

Observation of the co-eruptive ground deformation 6–7 km northwest of Shinmoe-dake's vent, identified it as being the location of the magma chamber, as opposed to being just beneath the vent (Kozono *et al*., 2013; Nakao *et al*., 2013; Ueda *et al*., 2013). Hence, the conduit, which connects the magma chamber and the vent, would, at least partly, have a slant, or horizontal, geometry. However, the steady conduit-flow model in the present study assumes a vertical geometry. The effects of such an inclined conduit on degassing processes are not well understood. We hypothesize here that the effect would depend on the depth at which such an inclined geometry is located. In cases where the non-vertical portion exists solely below the level at which volatiles start to exsolve, the geometrical modification is unlikely to have a significant effect on the efficiency of the gas escape. In contrast, the degassing efficiency would increase if the inclined portion is plumbed at a shallow level above the bubble nucleation, since the gas phase is likely to be concentrated on the upper side of the conduit wall, in a stratified manner above the liquid. Such a stratified flow of the gas phase along the conduit might be even more efficient than in perfectly vertical cases, as demonstrated in laboratory experiments by Palma *et al*. (2011), and, if this is the case, such a geometrical effect on the degassing efficiency can be parameterized into a permeability exponent, ω, in the present model. In this context, the conduit inclination does not essentially alter the present argument, which states that the transition in eruption style was caused by a co-eruptive decrease of pressure within the chamber. However, the amount of pressure decrease needed for the lava extrusion to cease could be reasonably affected by a modification of the conduit system. Quantitative considerations regarding the influence of conduit inclination on degassing processes will be considered in a future work.

4.4 Lateral gas escape

In the previous section, we first examined several cases in which a lateral gas escape was incorporated, but later focused on a case with a solely vertical escape. At present, however, in the case of Shinmoe-dake, this simplification is not directly justified from observational evidence. We

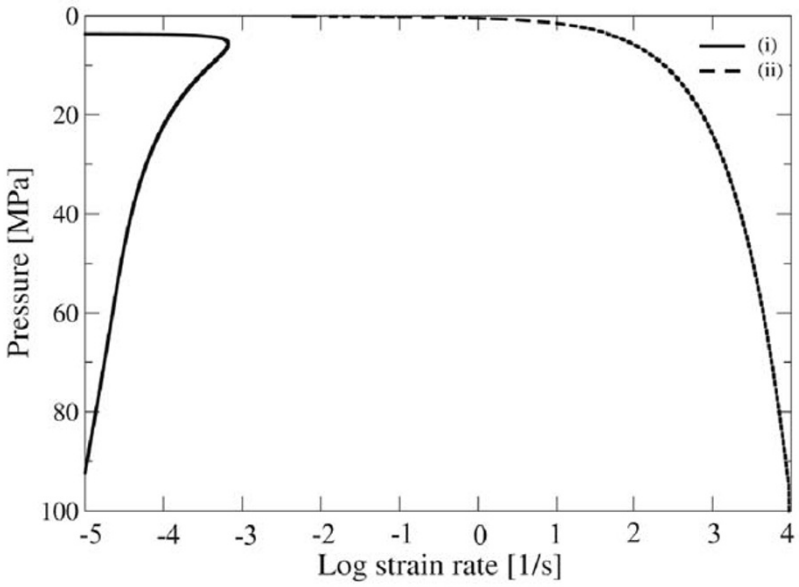

Fig. 7. Representative strain rate profile (i) and the profile of the critical value (ii) (right-hand-side of Eq. (11)) versus pressure along the conduit. Discharge rate = 87 m^3/s, R_c = 16 m, T = 980°C, n_0 = 4.0 wt%, L = 6 km, ω = 3.8, E_w = 0.

refer to the case of Mount Unzen, where a prolonged dome-forming eruption occurred in 1991–1995, and subsequent scientific drilling into the conduit was conducted in 2004. One of the important outcomes of the drilling was the discovery that a lateral gas escape across the conduit wall is not pronounced at a depth of 1.3 km. This is based on an observation of the drilled core that has a low permeability region around the conduit (Nakada *et al*., 2005). Although no magma-conduit system is identical between two volcanoes, our assumption that a vertical gas escape predominates, is supported. Considering again a stratified flow in an inclined conduit, however, the area of contact between the gas phase and the conduit wall might be larger than in a completely vertical case, and may invoke additional gas escape through the conduit wall. A quantitative evaluation of such an effect is beyond the scope of the present paper, although it requires future research.

4.5 Other possible effects on the termination of lava extrusion

In the previous section, we calculated the amount of reduction in magma chamber pressure required to cease the lava effusion. Here, we examine other effects on the termination of lava extrusion.

A change in the vent pressure due to loading of a lava dome is discussed in Melnik and Sparks (1999). We evaluate here the loading of a lava dome by applying excess pressure at the vent. Figure 8 shows how a change in the vent pressure alters the steady solution curve. In the figure we show two cases, in which 0.1 MPa (atmospheric) and 2.5 MPa (dome height of 100 m) are applied to the vent pressure. This reveals that the effect of lava loading appears only in a low discharge-rate region, and thus does not affect the behavior of the lava extrusion in the present discussion.

Wilson *et al*. (1980) discussed that conduit constriction due to downfaulting of the upper portion of the conduit wall would trigger a reduction in the discharge rate. It is, however, impossible to simulate the same situation in our model because it assumes a common conduit radius that is independent of depth. Instead, we evaluate here an effect of uniform expansion or shrink of the conduit, as already shown in Fig. 5(b). As expected, the narrowing of a conduit causes a decrease in the discharge rate. However, the pressure reduction required for the termination of lava effusion is not significantly dependent on the change in a conduit radius. Therefore, the conduit radius should become very narrow in order to stop the effusion. In addition, there are no observations of ground deformation which suggests such a collapse of the conduit. Accordingly, we do not consider that the shrink of the conduit radius is the cause of the termination of the effusive stage in Shinmoe-dake 2011 eruption.

4.6 Magma chamber volume

We estimate the magma chamber volume using the amount of pressure decrease deduced in the previous section. According to the Geospatial Information Authority of Japan (2012), the ground deformation around Shinmoe-dake can be modeled by a simple Mogi source. If a Mogi model is applied to the deflating ground deformation during the eruption, the volume change at the pressure source is represented as:

$$\Delta V = \frac{\pi a_0^3 \Delta P}{\nu}, \tag{12}$$

where ΔV and ΔP are the changes in volume and pressure of the magma chamber, respectively, and a_0 and ν are the radius of the spherical chamber and the rigidity of the host rock, respectively. Equation (12) can be rewritten with regard to ΔP as follows:

$$\Delta P = \frac{\nu \Delta V}{\pi a_0^3} = \frac{4\nu \Delta V}{3V}, \tag{13}$$

where V, in the term on the far right, represents the magma chamber volume. We then obtain the chamber volume by

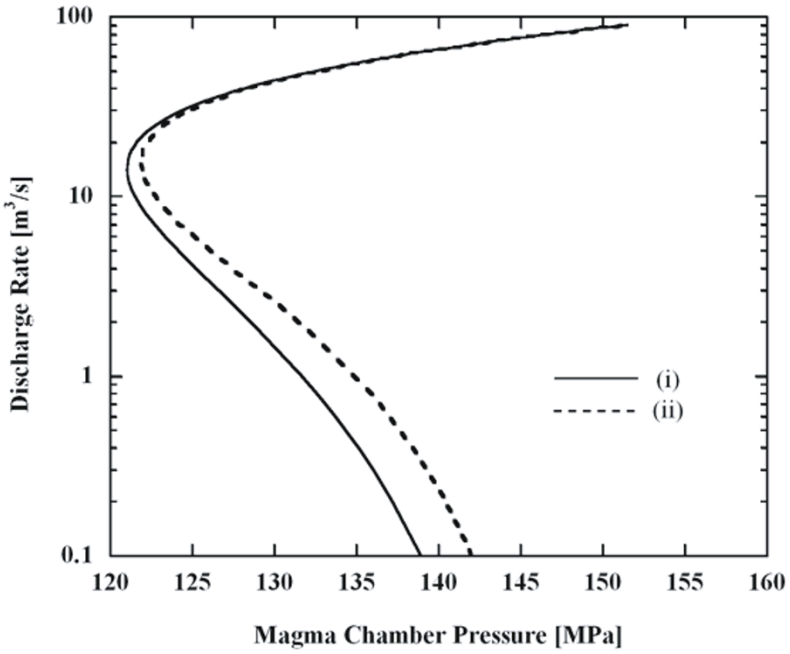

Fig. 8. Relation between the magma chamber pressure and discharge rate demonstrating an effect of loading by a lava dome. Parameters used for the calculations are $R_c = 16$ m, $T = 980^{\circ}$C, $n_0 = 4.0$ wt%, $L = 6$ km, $\omega = 3.8$, $E_w = 0$. The pressure at the vent for cases without a lava dome (i), and with a dome of 100 m high (ii), are atmospheric and 2.5 MPa, respectively.

rewriting Eq. (13) as follows:

$$V = \frac{4\nu\Delta V}{3\Delta P}. \tag{14}$$

Here, ΔP is the pressure reduction during the lava effusion which is estimated in the present study (3×10^7 Pa). If we apply a typical rigidity of the crust (3×10^{10} Pa) to ν, and assume that ΔV is equal to the volume change (5.3×10^6 m^3) at the magma chamber estimated by Kozono *et al*. (2013), in which the compressibility of bubble bearing magma is taken into account, the volume of Shinmoe-dake's magma chamber is estimated to be 7×10^9 m^3 from Eq. (14).

This volume corresponds to a sphere with a radius of approximately 1 km, which amounts to 500–600 times of the erupted volume. If all the space within the sphere is occupied by magma, this would be recognized as a remarkable seismic low-velocity anomaly. However, regional-scale seismic tomography by Wang and Zhao (2006), has not found such a low-velocity body. Although this may be attributed to the resolution of the tomography, the chamber volume we estimated may represent an upper limit. This may be because of (a) the rigidity of host rock adjacent to the magma chamber being possibly lower than that of the ordinary crust, (as a result of thermal softening), and (b) the co-eruptive replenishment of magma from below. If either of these reasons is the case, the deflation volume of the chamber, that is implied from the ground surface deformation, could be somewhat smaller than the erupted volume. A contribution of such mechanisms requires verification by further modeling and observations. It should be noted that the chamber volume that we estimated above also has a certain ambiguity depending on the resolution in source depth and shape of the deformation model, although the Mogi model that we used shows a general agreement with the GPS observations.

5. Conclusions

Using the 2011 eruption of Shinmoe-dake in which the eruption style underwent a transition from sub-plinian explosions to an extrusion of lava as an example, we investigated the conditions for the eruption to be effusive and for the effusive eruption to cease. The model of Kozono and Koyaguchi (2010), which incorporates both lateral and vertical degassing, enables us to obtain the contour maps of the permeability exponent as Fig. 4, and to evaluate the condition in which the eruption style becomes effusive. In order for the magma flowing along the conduit not to be fragmented, ω the permeability exponent, should be greater than 3.7 under a conduit radius of 16 m, for a discharge rate corresponding to the observed one when lateral gas escape was absent. According to our calculations, the termination of lava extrusion seems to have been brought about by a successive reduction of the chamber pressure. The estimated amount of pressure decrement until the termination of lava extrusion is 3×10^7 Pa. Applying a Mogi model, we then infer the total volume of the magma chamber as being 1×10^{10} m^3. Considering no significant low-velocity body has been reported at the pressure source, (at least not in the preceding literature), our estimation of the chamber volume might be regarded as the upper limit.

Regarding the cause of the transition from sub-plinian to effusive eruptions, a reduction of the water content in the magma chamber is unlikely to have been the dominant cause, as certain petrological studies have uncovered no significant changes in the mineral composition. We propose

instead that a jump took place in the phase space between the chamber pressure and the mass flow rate in the magma-conduit system, in which multiple steady solutions are expected. This should be confirmed in a further study which can deal with both explosive and effusive eruptions within a single framework.

Acknowledgments. We sincerely thank Drs. Tomofumi Kozono and Yuki Suzuki for their comments that helped improve the manuscript. We are grateful to Dr. Mie Ichihara and two reviewers for helpful comments and suggestions that greatly improved the manuscript.

References

Barmin, A., O. Melnik, and R. S. J. Sparks, Periodic behavior in lava dome eruptions, *Earth Planet. Sci. Lett.*, **199**, 173–184, 2002.

Dingwell, D. B. and S. Webb, Structural relaxation in silicate melts and non-Newtonian melt rheology in geological processes, *Phys. Chem. Miner.*, **16**, 508–516, 1989.

Eichelberger, J., C. Carrigan, H. Westrich, and R. Price, Non-explosive silicic volcanism, *Nature*, **323**, 598–602, 1986.

Geospatial Information Authority of Japan, Crustal deformation around Kirishima Volcano, *Rep. Coord. Comm. Predict. Volcan. Erup.*, **108**, 197–220, 2012.

Imura, R. and T. Kobayashi, Geological map of Kirishima Volcano, 1:50,000, *Geological Map of Volcanoes*, **11**, Geological survey of Japan, 2001.

Jaupart, C. and C. Allegre, Gas content, eruption rate and instabilities of eruption regime in silicic volcanoes, *Earth Planet. Sci. Lett.*, **102**, 413–429, 1991.

Kozono, T. and T. Koyaguchi, Effects of relative motion between gas and liquid on 1-dimensional steady flow in silicic volcanic conduit: 1. an analytical method, *J. Volcanol. Geotherm. Res.*, **180**, 21–36, 2009.

Kozono, T. and T. Koyaguchi, A simple formula for calculating porosity of magma in volcanic conduit during dome-forming eruptions, *Earth Planets Space*, **62**, 483–488, 2010.

Kozono, T., H. Ueda, T. Ozawa, T. Koyaguchi, E. Fujita, A. Tomiya, and Y. J. Suzuki, Magma discharge variations during the 2011 eruptions of Shinmoe-dake volcano, Japan, revealed by geodetic and satellite observations, *Bull. Volcanol.*, doi:10.1007/s00445-013-0695-4, 2013.

Melnik, O. and R. S. J. Sparks, Nonlinear dynamics of lava dome extrusion, *Nature*, **402**, 37–41, 1999.

Mueller, S., O. Melnik, O. Spieler, B. Scheu, and D. B. Dingwell, Permeability and degassing of lavas undergoing rapid decompression: An experimental determination, *Bull. Volcanol.*, **67**, 526–538, 2005.

Nakada, S., K. Uto, S. Sakuma, J. C. Eichelberger, and H. Shimizu, Scientific results of conduit drilling in the Unzen Scientific Drilling Project (USDP), *Sci. Drill.*, **1**, 18–22, 2005.

Nakada, S., M. Nagai, T. Kaneko, Y. Suzuki, and F. Maeno, The outline of the 2011 eruption at Shinmoe-dake (Kirishima), Japan, *Earth Planets Space*, **65**, this issue, 475–488, doi:10.5047/eps.2013.03.016, 2013.

Nakao, S., Y. Morita, H. Yakiwara, J. Oikawa, H. Ueda, H. Takahashi, Y. Ohta, T. Matsushima, and M. Iguchi, Volume change of the magma reservoir relating to the 2011 Kirishima Shinmoe-dake eruption—Charging, discharging and recharging process inferred from GPS measurements, *Earth Planets Space*, **65**, this issue, 505–515, doi:10.5047/eps.2013.05.017, 2013.

Palma, J. L., S. Blake, and E. S. Calder, Constraints on the rates of degassing and convection in basaltic open-vent volcanoes, *Geochem. Geophys. Geosyst.*, **12**, Q11006, doi:10.1029/2011GC003715, 2011.

Papale, P., Strain-induced magma fragmentation in explosive eruptions, *Nature*, **397**, 452–428, 1999.

Proussevitch, A. A., D. L. Sahagian, and A. T. Anderson, Dynamics of diffusive bubble growth in magmas: Isothermal case, *J. Geophys. Res.*, **98**, 17447–17455, 1993.

Slezin, Y., The mechanism of volcanic eruptions (a steady state approach), *J. Volcanol. Geotherm. Res.*, **122**, 7–50, 2003.

Suzuki, Y., A. Yasuda, N. Hokanishi, T. Kaneko, S. Nakada, and T. Fujii, Syneruptive deep magma transfer and shallow magma remobilization during the 2011 eruption of Shinmoe-dake, Japan—Constraints from melt inclusions and phase equilibria experiments—, *J. Volcanol. Geotherm. Res.*, **257**, 184–204, 2013.

Tsutsui, M., K. Tomita, and T. Kobayashi, Fumarolic activity since December 2003 and volcanic activity during the Meiji and Taisho eras (1880–1923) of Ohachi Volcano, Kishirima Volcano Group, Southern Kyushu, Japan, *Bull. Volcanol. Soc. Jpn.*, **50**, 475–489, 2005 (in Japanese with English abstract).

Ueda, H., T. Kozono, E. Fujita, Y. Kohno, M. Nagai, Y. Miyagi, and T. Tanada, Crustal deformation associated with the 2011 Shinmoe-dake eruption as observed by tiltmeters and GPS, *Earth Planets Space*, **65**, this issue, 517–525, doi:10.5047/eps.2013.03.001, 2013.

Wang, Z. and D. Zhao, Vp and Vs tomography of Kyushu, Japan: New insight into arc magmatism and forearc seismotectonics, *Phys. Earth Planet. Inter.*, **157**, 269–285, 2006.

Webb, S. and D. Dingwell, Non-Newtonian rheology of igneous melts at high stress and strain rate: Experimental results for rhyolite, andesite basalt and nephelinite, *J. Geophys. Res.*, **95**, 15695–15701, 1990.

Wilson, L., R. Sparks, and G. Walker, Explosive volcanic eruptions: IV. The control of magma properties and conduit geometry on eruption column behavior, *Geophys. J. R. Astron. Soc.*, **63**, 117–148, 1980.

Woods, A. and T. Koyaguchi, Transitions between explosive and effusive eruptions of silicic magmas, *Nature*, **370**, 641–644, 1994.

Yoshida, S. and T. Koyaguchi, A new regime of volcanic eruption due to the relative motion between liquid and gas, *J. Volcanol. Geotherm. Res.*, **89**, 303–315, 1999.

R. Tanaka (e-mail: ryo-10@mail.sci.hokudai.ac.jp) and T. Hashimoto